Earth and Planetary Science Letters 286 (2009) 198–207

Contents lists available at ScienceDirect

Earth and Planetary Science Letters

journal homepage: www.elsevier.com/locate/epsl

Water mass exchange and variations in seawater temperature in the NW Tethys during the Early Jurassic: Evidence from neodymium and oxygen isotopes of fish teeth and belemnites

Guillaume Dera [a,*], Emmanuelle Pucéat [a], Pierre Pellenard [a], Pascal Neige [a], Dominique Delsate [b], Michael M. Joachimski [c], Laurie Reisberg [d], Mathieu Martinez [a]

[a] UMR CNRS 5561 Biogéosciences, Université de Bourgogne, 6 bd Gabriel, 21000 Dijon, France
[b] Muséum National d'Histoire Naturelle, 25 rue Münster, 2160 Luxembourg, Luxemburg
[c] GeoZentrum Nordbayern, Universität Erlangen-Nürnberg, Schlossgarten 5, 91054 Erlangen, Germany
[d] Centre de Recherches Pétrographiques et Géochimiques (CRPG), Nancy-Université, CNRS, 15 rue Notre Dame des Pauvres, 54501 Vandoeuvre lès Nancy, France

ARTICLE INFO

Article history:
Received 2 December 2008
Received in revised form 17 June 2009
Accepted 21 June 2009
Available online 16 July 2009

Editor: M.L. Delaney

Keywords:
paleoclimate
paleoceanography
neodymium isotopes
oxygen isotopes
fish tooth
Toarcian

ABSTRACT

Oxygen and neodymium isotope analyses performed on biostratigraphically well-dated fish remains recovered from the Hettangian to Toarcian of the Paris Basin were used to reconstruct variations of Early Jurassic seawater temperature and to track oceanographic changes in the NW Tethys. Our results indicate a strong correlation between $\delta^{18}O$ trends recorded by fish remains and belemnites, confirming the paleoenvironmental origin of oxygen isotope variations. Interestingly, temperatures recorded by pelagic fishes and nektobenthic belemnites and bottom dwelling fishes are comparable during the Late Pliensbachian sea-level lowstand but gradually differ during the Early Toarcian transgressive episode, recording a difference in water temperatures of ~6 °C during the Bifrons Zone. This could suggest that the surface-bottom water temperature difference was not large enough during regressive phases to be recorded by organisms living near the lower and upper part of the water column. The globally unradiogenic Nd budget of Euro-boreal waters through the Early Jurassic suggests that these waters were strongly affected by continental neodymium input from surrounding emerged areas and that exchange with more radiogenic waters from the Tethys and Panthalassa oceans remained limited. This supports the existence of a southward directed current in the Euro-boreal area for most of the Early Jurassic. The only exception is observed at the Early–Late Pliensbachian transition where a positive ε_{Nd} excursion is recorded, suggesting northward influx of low-latitude Tethyan or Panthalassan waters which may have contributed to the warming of NW Tethyan seawater recorded at this time. The absence of a marked negative excursion in ε_{Nd} concomitant with a negative $\delta^{18}O$ shift recorded during the Falciferum Zone (Exaratum Subzone) argues against the influence of less radiogenic Arctic water influxes with low $\delta^{18}O$ values during this interval. Instead, we suggest that enhanced freshwater inputs related to increasing weathering rates could have contributed to the large $\delta^{18}O$ shift recorded by marine organisms, especially in Euro-boreal contexts.

1. Introduction

Early Jurassic times (~200–175 Ma, Gradstein et al., 2004) were marked by a 2nd order biodiversity crisis (Little and Benton, 1995) and perturbations of the carbon cycle documented by $\delta^{13}C$ excursions and organic-rich deposits (Jenkyns, 1988; Röhl et al., 2001; Hesselbo et al., 2007; Hermoso et al., 2009). Several recent studies link these environmental changes to paleoceanographic disturbances (van de Schootbrugge et al., 2005b), episodes of clathrate destabilisation (Hesselbo et al., 2000a; Beerling et al., 2002), thermogenic methanogenesis or volcanism in the Karoo–Ferrar Large Igneous Province (McElwain et al., 2005; Svensen et al., 2007) (Fig. 1), having potentially triggered climatic variations during the Early Jurassic (Gómez et al., 2008). Available oxygen isotope data point to a warming of seawater at the end of the Early Pliensbachian, cooling during the Late Pliensbachian, followed by a prominent warming during the Early–Middle Toarcian (McArthur et al., 2000; Bailey et al., 2003; Rosales et al., 2004; van de Schootbrugge et al., 2005a; Gómez et al., 2008).

The paleoclimatic data are almost exclusively based on $\delta^{18}O$ analyses of belemnite guards which are particularly abundant in the Sinemurian, Pliensbachian, and Toarcian. However, the use of belemnite $\delta^{18}O$ data as sea surface temperature proxies may be questioned due to uncertainties concerning the habitat of these

* Corresponding author. Present address: Université de Bourgogne, Laboratoire Biogéosciences, 6 bd Gabriel, 21000 Dijon, France. Tel.: +33 3 80 39 37 69; fax: +33 3 80 39 63 87.
E-mail address: guillaume.dera@u-bourgogne.fr (G. Dera).

0012-821X/$ – see front matter © 2009 Elsevier B.V. All rights reserved.
doi:10.1016/j.epsl.2009.06.027

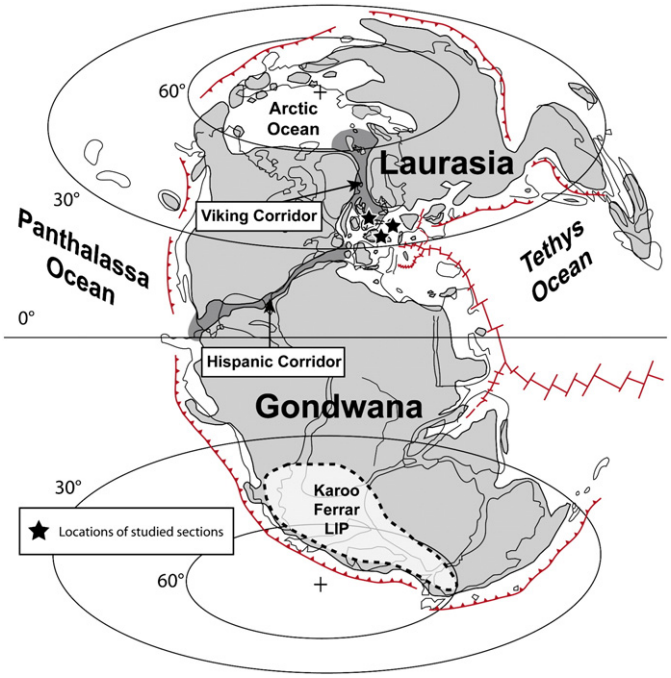

Fig. 1. Paleogeographic reconstruction for the Pliensbachian–Toarcian period (modified from Damborenea, 2002).

coleoids. Recent geochemical studies suggest that belemnites likely inhabited intermediate to deep waters (van de Schootbrugge et al., 2000; Dutton et al., 2007; Wierzbowski and Joachimski, 2007), but could have migrated in the water column during their lifespan (Zakharov et al., 2006). In addition, the habitat and vital fractionation effects during calcite precipitation could vary according to species (McArthur et al., 2007). As there was an important turnover in the belemnite fauna during the Pliensbachian to Toarcian (Doyle, 1994), changes in analysed belemnite species may introduce a bias in the isotope record. There is therefore a need for additional biological materials for isotopic analysis for which life environment and fractionation processes are better constrained.

Until today, Early Jurassic oxygen isotope records are only available from European basins that represent the north-western epicontinental sea of the Peritethyan area. As these regions were located at the convergence of the "Viking" and "Hispanic" corridors connecting the Arctic and Panthalassa oceans to the north-western Tethys Ocean (Fig. 1), water mass exchange between these basins may have influenced both sea surface temperature and salinity in the NW Tethys (Saelen et al., 1996; van de Schootbrugge et al., 2005a). In particular, large freshwater inputs have been invoked to explain the decrease in calcite $\delta^{18}O$ values during the Early Toarcian (Bailey et al., 2003; Suan et al., 2008). However, further paleoceanographic data are needed to differentiate between global and local temperature changes and regional $\delta^{18}O_{seawater}$ variations.

In this study, we reconstruct the evolution of Early Jurassic seawater temperature and attempt to track oceanographic changes in the NW Tethys using oxygen and neodymium isotopes measured from fish teeth recovered from the Hettangian to Toarcian of the Paris Basin. In addition, belemnite rostra from the same stratigraphic levels were analysed for their oxygen isotope composition, in order to compare fish tooth and belemnite $\delta^{18}O$ signals. Fish tooth $\delta^{18}O$ is a robust temperature proxy because fish paleoecology can be inferred from tooth morphology (Cappetta, 1987), and because apatite is relatively resistant to diagenetic alteration and presents a unique fractionation equation for oxygen applicable to all fish species (Kolodny et al., 1983; Lécuyer et al., 1999; Vennemann et al., 2001). In addition, the neodymium isotope composition (ε_{Nd}) of fish tooth apatite is usually considered as a reliable proxy for tracking changes in oceanic circulation (e.g., Grandjean et al., 1988; Vennemann and Hegner, 1998; Thomas et al., 2003; Pucéat et al., 2005). As continental weathering is the principal source of Nd to the oceans, the Nd isotope system is also a potential proxy for constraining erosional inputs to basins (Jones et al., 1994, Reynolds et al. 2006). Thus, combined oxygen and neodymium isotope analyses of fish teeth should provide a better understanding of the origin of $\delta^{18}O$ variations recorded by belemnites during the Early Jurassic.

2. Material and sampling

Nearly 150 fish remains, consisting of macroteeth (>1 mm), microteeth (<1 mm), and scales were hand-picked from Hettangian to Toarcian sediments from Belgian, French, and Luxembourgian parts of the Paris Basin (Fig. 2). Thirty belemnite guards from the same beds were also studied in order to compare their $\delta^{18}O$ signals to those of the fish teeth. Sedimentological data (marly to sandy lithologies) indicate that shallow-marine coastal conditions prevailed during the Hettangian to Sinemurian, whereas deeper and open-marine conditions not exceeding 200 m of depth (evidenced by marly to muddy facies with only sporadic sandy sediments) characterized the Pliensbachian–Toarcian interval (Boulvain et al., 2000). Fish teeth from the Worcester Basin (England) and the western part of the Paris Basin (Sarthe, France) were studied for comparison. All analysed fossil hard parts were biostratigraphically dated down to the ammonite zone and subzone level.

Fish remains were taxonomically determined and assigned to a specific habitat (pelagic or demersal) using the selachian tooth typology of Cappetta (1987) (Fig. 3; Table 1). Samples comprised widespread Early Jurassic fauna including chondrichthyans (sharks, rays) and actinopterygians (Rees, 2000; Delsate, 2003). As fish teeth mineralize over several weeks to several months depending on species, fish tooth $\delta^{18}O$ values from a certain stratigraphic level often show some scatter because of vertical or horizontal migration of the fishes and seasonal variations in seawater temperature. In order to minimize this variation, several microteeth of the same species and recovered from the same horizon were combined in a single sample for analysis (see Table 1). Except in the case of the smallest teeth, enamel was separated from dentine for oxygen isotope analyses. For ε_{Nd} analyses, both dentine and enamel of the largest samples were analysed together.

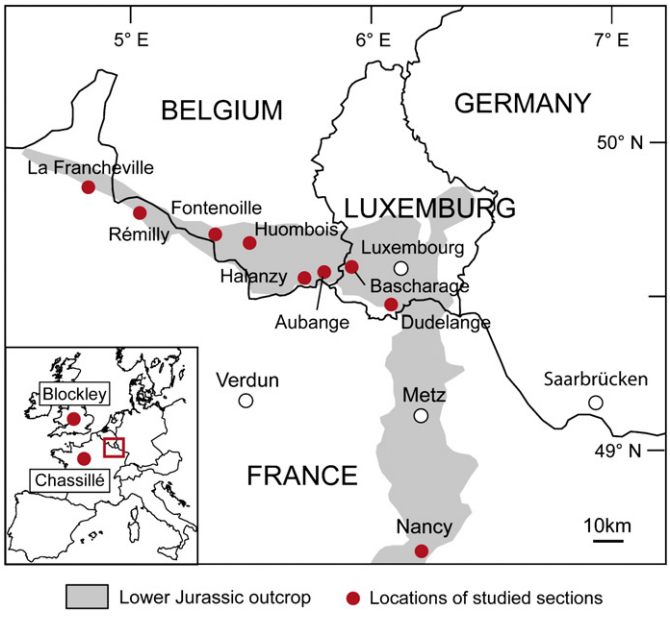

Fig. 2. Locations of studied sections.

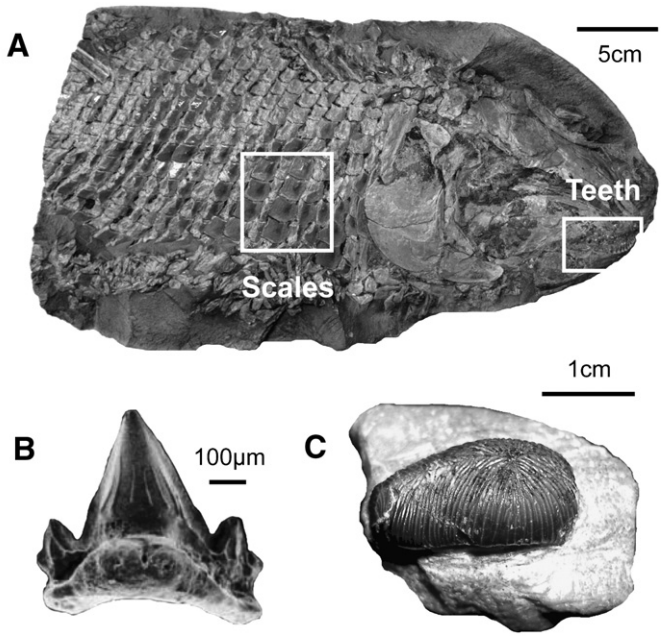

Fig. 3. Examples of fish remains used for $\delta^{18}O$ and ε_{Nd} analyses. (A) Scales and microteeth of *Lepidotes elvensis* (inventory number UBGD 276166). (B) Clutching-type microtooth of pelagic *Synechodus streitzi*. (C) Grinding-type macrotooth of demersal *Acrodus nobilis*.

Thirty belemnite guards were taxonomically determined according to the classification of Doyle (1990), including representatives of the genera *Acrocoelites*, *Dactyloteuthis*, and *Passaloteuthis* (Table 2). The rostra were sectioned along the length, polished, and investigated using cathodoluminescence microscopy in order to identify diagenetic recrystallisation. Luminescent and non-luminescent areas of each rostrum were accurately mapped in order to sample exclusively the non-luminescent parts for stable isotope analysis. In order to average potential intra-rostral variability in $\delta^{18}O$ related to migration and seasonality, several samples were taken from individual rostra. The drilled powders were combined and homogenized prior to analysis.

3. Analytical procedures

Stable isotope analyses were performed at the GeoZentrum Nordbayern of the University of Erlangen-Nuremberg (Germany). Thirty-five apatite samples (0.5 to 1 mg) were dissolved in nitric acid and chemically converted to Ag_3PO_4 using a modified version of the method described by O'Neil et al. (1994). Oxygen isotope ratios were measured on CO using a High Temperature Conversion Elemental Analyzer (TC-EA) connected online to a ThermoFinnigan Delta plus mass spectrometer (for details see Joachimski et al. (2004)). All $\delta^{18}O_{apatite}$ values are reported in per mil relative to V-SMOW (Vienna Standard Mean Ocean Water). Accuracy and reproducibility (better than $\pm 0.2‰$) were monitored by multiple analyses of trisilverphosphate from NBS120c and several trisilverphosphate standards (TUI-1, TUI-2, YR-2; Vennemann et al., 2002). The average oxygen isotope compositions of TUI-1, TUI-2 and YR-2 standards were 21.3, 5.5, and 13.2‰ V-SMOW, respectively. The mean $\delta^{18}O$ value of NBS120c was 22.7‰ V-SMOW, which is relatively close to the value of 22.6‰ V-SMOW determined by Vennemann et al. (2002).

Belemnite carbonate powders were reacted with 100% phosphoric acid at 75 °C using a Kiel III online carbonate preparation line connected

Table 1
Locations, biostratigraphy, taxonomy, oxygen isotope compositions, and calculated seawater temperatures of fish remains.

Sample	Location	Stage	Biozone	Subzone	$\delta^{18}O$ (‰ SMOW)	Temperature (°C)	Taxonomy	Number of specimens	Ecology
He1	Fontenoille (B)	Hettangian	*liasicus*	–	20.65	18.5	*Hybodus reticulatus*	1	d
He2	Fontenoille (B)	Hettangian	*liasicus*	–	20.78	17.9	*Hybodus reticulatus*	1	d
He3	Fontenoille (B)	Hettangian	*liasicus*	–	21.17	16.2	*Hybodus reticulatus*	1	d
He4	Fontenoille (B)	Hettangian	*liasicus*	–	21.14	16.3	*Synechodus streitzi*	3	p
Se1a	Huombois (B)	Sinemurian	*semicostatum*	–	19.91	21.7	*Acrodus nobilis*	1	d
Da1a	Francheville (F)	Pliensbachian	*davoei*	*figulinum*	19.85	22.0	Undetermined	1	d
Ma1a	Rémilly (F)	Pliensbachian	*margaritatus*	*stokesi*	20.92	17.3	*Synechodus* sp.	3	p
Ma2a	Rémilly (F)	Pliensbachian	*margaritatus*	*stokesi*	19.84	22.0	*Actinopterygia*	5	p
Ma2b	Rémilly (F)	Pliensbachian	*margaritatus*	*stokesi*	20.58	18.8	*Actinopterygia*	3	p
Sp1a	Aubange (B)	Pliensbachian	*spinatum*	*hawskerense*	22.36	11.0	*Synechodus* sp.	2	p
Sp1b	Aubange (B)	Pliensbachian	*spinatum*	*hawskerense*	21.14	16.3	*Synechodus* sp.	2	p
Sp2a	Aubange (B)	Pliensbachian	*spinatum*	*hawskerense*	22.51	10.3	*Synechodus* sp.	5	p
Te1a	Aubange (B)	Toarcian	*tenuicostatum*	*semicelatum*	19.89	21.8	*Synechodus* sp.	1	p
Te1b	Aubange (B)	Toarcian	*tenuicostatum*	*semicelatum*	19.79	22.2	*Synechodus* sp.	1	p
Te3a	Aubange (B)	Toarcian	*tenuicostatum*	*semicelatum*	20.24	20.3	*Welcomia terencei*	1	p
Fa3a	Bascharage (L)	Toarcian	*falciferum*	*exaratum*	17.96	30.3	*Lepidotes elvensis*	4	p
Fa3b	Bascharage (L)	Toarcian	*falciferum*	*exaratum*	17.32	33.1	*Lepidotes elvensis*	2	p
Fa1a	Nancy (F)	Toarcian	*falciferum*	*falciferum*	18.43	28.2	*Hybodus hauffianus*	5	d
Fa2b	Nancy (F)	Toarcian	*falciferum*	*falciferum*	18.96	25.9	*Hybodus hauffianus*	2	d
Bi1a	Halanzy (B)	Toarcian	*bifrons*	*crassum*	19.09	25.3	*Actinopterygia*	4	p
Bi1b	Halanzy (B)	Toarcian	*bifrons*	*crassum*	20.67	18.4	*Actinopterygia*	2	p
Bi1c	Halanzy (B)	Toarcian	*bifrons*	*crassum*	19.48	23.6	*Actinopterygia*	3	p
Bi2a	Halanzy (B)	Toarcian	*bifrons*	*crassum*	20.27	20.1	*Hemiscylliidae*	4	d
Bi2b	Halanzy (B)	Toarcian	*bifrons*	*crassum*	20.94	17.2	*Hemiscylliidae*	5	d
Bi2c	Halanzy (B)	Toarcian	*bifrons*	*crassum*	19.59	23.1	*Hemiscylliidae*	6	d
Bi2d	Halanzy (B)	Toarcian	*bifrons*	*crassum*	20.31	20.0	*Hemiscylliidae*	5	d
Bi3a	Halanzy (B)	Toarcian	*bifrons*	*crassum*	19.12	25.2	Synechodontiform	1	p
Bi3b	Halanzy (B)	Toarcian	*bifrons*	*crassum*	18.38	28.4	Synechodontiform	1	p
Bi4a	Halanzy (B)	Toarcian	*bifrons*	*crassum*	20.7	18.3	*Toarcibatis* sp.	15	d
Bi5a	Halanzy (B)	Toarcian	*bifrons*	*crassum*	20.62	18.6	*Paleobrachaelurus* sp.	8	d
Bi5b	Halanzy (B)	Toarcian	*bifrons*	*crassum*	20.41	19.5	*Paleobrachaelurus* sp.	7	d
Le1a	Dudelange (L)	Toarcian	*Aalensis*	–	18.91	26.1	*Rhomphaiodon* sp.	4	p
Le1b	Dudelange (L)	Toarcian	*Aalensis*	–	19.14	25.1	*Rhomphaiodon* sp.	2	p
Le1c	Dudelange (L)	Toarcian	*Aalensis*	–	18.91	26.1	*Rhomphaiodon* sp.	3	p
Le2a	Dudelange (L)	Toarcian	*Aalensis*	–	17.51	32.2	*Batomorphii* sp.	2	d

B — Belgium, L — Luxemburg, F — France, p — pelagic, d — demersal.

Table 2
Locations, biostratigraphy, taxonomy, oxygen and carbon isotope compositions, and calculated seawater temperatures of belemnites.

Sample	Location	Stage	Biozone	Subzone	$\delta^{18}O$ (‰ PDB)	$\delta^{13}C$ (‰ PDB)	Temperatures (°C)	Taxonomy
BDB	Aubange (B)	Pliensbachian	*spinatum*	*hawskerense*	0.64	0.67	9.5	*Passaloteuthididae*
BDC	Aubange (B)	Pliensbachian	*spinatum*	*hawskerense*	0.73	−1.36	9.2	*Passaloteuthididae*
BDA	Aubange (B)	Pliensbachian	*spinatum*	*hawskerense*	0.26	1.91	11.0	*Passaloteuthis* sp.
BAA	Aubange (B)	Toarcian	*tenuicostatum*	*semicelatum*	−0.70	2.09	14.8	*Passaloteuthis milleri*
BAB	Aubange (B)	Toarcian	*tenuicostatum*	*semicelatum*	−1.34	3.83	17.4	*Passaloteuthis milleri*
BAD	Aubange (B)	Toarcian	*tenuicostatum*	*semicelatum*	−0.79	1.79	15.1	*Passaloteuthis milleri*
BAE	Aubange (B)	Toarcian	*tenuicostatum*	*semicelatum*	−2.24	2.50	21.3	*Passaloteuthis milleri*
BAC	Aubange (B)	Toarcian	*tenuicostatum*	*semicelatum*	−1.54	0.54	18.3	*Passaloteuthis* sp.
BBA	Aubange (B)	Toarcian	*falciferum*	*exaratum*	−2.35	2.99	21.8	*Acroelites (Toarcibelus) ilmensterensis*
BEB	Halanzy (B)	Toarcian	*bifrons*	*crassum*	−2.20	2.06	21.1	*Acrocoelites (Acroelites)* sp.
BCA	Halanzy (B)	Toarcian	*bifrons*	*crassum*	−1.13	0.66	16.5	*Acrocoelites (Acroelites)* sp.
BCC	Halanzy (B)	Toarcian	*bifrons*	*crassum*	−1.42	0.09	17.8	*Acrocoelites (Acroelites)* sp.
BCD	Halanzy (B)	Toarcian	*bifrons*	*crassum*	−1.04	−0.05	16.2	*Acrocoelites (Acroelites)* sp.
BCF	Halanzy (B)	Toarcian	*bifrons*	*crassum*	−3.21	2.20	25.8	*Acrocoelites (Acroelites)* sp.
BCI	Halanzy (B)	Toarcian	*bifrons*	*crassum*	−1.42	0.44	17.8	*Acrocoelites (Acroelites)* sp.
BCJ	Halanzy (B)	Toarcian	*bifrons*	*crassum*	−0.67	2.03	14.6	*Acrocoelites (Acroelites)* sp.
BCK	Halanzy (B)	Toarcian	*bifrons*	*crassum*	−1.25	−0.41	17.1	*Acrocoelites (Acroelites)* sp.
BCL	Halanzy (B)	Toarcian	*bifrons*	*crassum*	−1.29	0.37	17.2	*Acrocoelites (Acroelites)* sp.
BCM	Halanzy (B)	Toarcian	*bifrons*	*crassum*	−1.35	−0.28	17.5	*Acrocoelites (Acroelites)* sp.
BCP	Halanzy (B)	Toarcian	*bifrons*	*crassum*	−1.15	0.86	16.6	*Acrocoelites (Acroelites)* sp.
BCQ	Halanzy (B)	Toarcian	*bifrons*	*crassum*	−2.04	1.92	20.5	*Acrocoelites (Acroelites)* sp.
BCR	Halanzy (B)	Toarcian	*bifrons*	*crassum*	−1.22	0.11	16.9	*Acrocoelites (Acroelites)* sp.
BEE	Halanzy (B)	Toarcian	*bifrons*	*crassum*	−0.89	0.20	15.6	aff. *Dactyloteuthis*
BEA	Halanzy (B)	Toarcian	*bifrons*	*crassum*	−1.89	1.34	19.8	*Dactyloteuthis digitalis*
BEC	Halanzy (B)	Toarcian	*bifrons*	*crassum*	−1.69	−0.12	18.9	*Dactyloteuthis* sp.
BED	Halanzy (B)	Toarcian	*bifrons*	*crassum*	−1.38	0.85	17.6	*Dactyloteuthis* sp.
BEF	Halanzy (B)	Toarcian	*bifrons*	*crassum*	−1.11	0.51	16.5	*Dactyloteuthis* sp.
BEG	Halanzy (B)	Toarcian	*bifrons*	*crassum*	−1.21	0.76	16.9	*Dactyloteuthis* sp.
BEH	Halanzy (B)	Toarcian	*bifrons*	*crassum*	−1.55	1.21	18.3	*Dactyloteuthis* sp.

to a ThermoFinnigan 252 mass spectrometer. All values are reported in per mil relative to V-PDB by assigning a $\delta^{13}C$ value of +1.95‰ and a $\delta^{18}O$ value of −2.20‰ to NBS19. Reproducibility was checked by replicate analysis of laboratory standards and is ±0.02 (1σ) for $\delta^{13}C$ and ±0.04 (1σ) for $\delta^{18}O$.

Neodymium isotope analyses of eleven apatite powders were performed at the CRPG-CNRS laboratory in Nancy, France. After addition of a mixed ^{150}Nd–^{147}Sm spike, from 13 to 57 mg of sample powder were dissolved in 6 N HCl, then evaporated to dryness and redissolved in 1 ml of 2.5 N HCl. Nd and Sm were separated by standard cation exchange techniques following the protocol described in Pucéat et al. (2005). Nd and Sm isotope analyses were performed on a Finnigan MAT 262 mass spectrometer in dynamic multicollection mode. Nd was run as a metal on a double Re–Ta filament using a P_2O_5 activator. Approximately 90 isotopic ratios were collected for each sample. Nd isotope ratios were corrected for mass discrimination by normalizing to $^{143}Nd/^{144}Nd = 0.7219$ using an exponential law. In-run uncertainties on the $^{143}Nd/^{144}Nd$ ratios were, on average, 0.000015, and were always less than or equal to 0.000022 (2 standard errors, see Table 3). During the period of measurement, the value of the La Jolla Nd standard was 0.511841 ±0.000020 (2σ, $n = 20$). Total Nd blanks were less than 500 pg, and were thus negligible relative to the quantities of Nd analyzed. Unfortunately, due to underspiking, reliable Sm and Nd concentration results were obtained from only two samples (SM and CH). For the other samples, a $^{147}Sm/^{144}Nd$ ratio of 0.118 ± 0.036 (2σ) was assumed for calculation of the initial $^{143}Nd/^{144}Nd$ ratios, based on literature Sm and Nd concentrations (Grandjean et al., 1987, 1988; Vennemann and Hegner, 1998; Picard et al., 2002; Thomas et al., 2003; Lécuyer et al., 2004; Scher and Martin, 2004). Final results are reported in $\varepsilon_{Nd(T)}$ notation relative to the CHUR mantle evolution curve (see Table 3 for details). The relatively large uncertainty of most initial Nd compositions (±0.4 to ±0.9 epsilon units) reflects the uncertainty on the age correction caused by the poor constraint of the $^{147}Sm/^{144}Nd$ ratio.

Table 3
Locations, biostratigraphy, ages and Nd isotope compositions of Early Jurassic fish remains.

Sample	Location	Stage	Biozone	Subzone	Age (Ma)	Quantity analysed (mg)	$^{147}Sm/^{144}Nd$	$^{143}Nd/^{144}Nd$	$\varepsilon_{Nd(T)}$
Se3a	Huombois (B)	Sinemurian	*semicostatum*	Not specified	194.5	15.58	0.118	0.512080 ± 20	−8.9
BL	Blockley (E)	Pliensbachian	*ibex*	Not specified	188	not measured	0.118	0.512404 ± 14	−9.1
Da1b	Francheville (F)	Pliensbachian	*davoei*	*figulinum*	187	46.8	0.118	0.512223 ± 19	−6.2
Ma1b	Rémilly (F)	Pliensbachian	*margaritatus*	*stokesi*	186.5	29.54	0.118	0.512187 ± 19	−6.9
SM2	Nancy (F)	Pliensbachian	*margaritatus*	*subnodosus* or *gibbosus*	185.5	not measured	0.110	0.512399 ± 13	−9.3
CH2	Chassillé (F)	Pliensbachian	*spinatum*	*hawskerense*	185	not measured	0.120	0.512399 ± 6	−10
Te2a	Aubange (B)	Toarcian	*tenuicostatum*	*semicelatum*	183	15.46	0.118	0.512034 ± 22	−10
Fa3d	Bascharage (L)	Toarcian	*falciferum*	*exaratum*	182.5	56.59	0.118	0.512007 ± 11	−10.5
Bi2e	Halanzy (B)	Toarcian	*bifrons*	*crassum*	181	12.89	0.118	0.512076 ± 11	−9.1
Bi1d	Halanzy (B)	Toarcian	*bifrons*	*crassum*	181	40.98	0.118	0.512064 ± 21	−9.4
Le1d	Dudelange (L)	Toarcian	*aalensis*	Not specified	176	22.52	0.118	0.512043 ± 15	−9.8

$\varepsilon_{Nd(T)} = [(^{143}Nd/^{144}Nd)_{sample}/(^{143}Nd/^{144}Nd)_{CHUR} - 1] \times 10^4$, where CHUR is the Chondritic Uniform Reservoir and the isotopic ratios are the initial ratios at the time of deposition. Ages are from Gradstein et al. (2004). The initial $(^{143}Nd/^{144}Nd)_{CHUR}$ was calculated using a $^{147}Sm/^{144}Nd$ ratio of 0.1967, and a present-day $(^{143}Nd/^{144}Nd)_{CHUR}$ ratio of 0.512638. For most samples, $\varepsilon_{Nd(T)}$ values were calculated assuming a $^{147}Sm/^{144}Nd$ value of 0.118, based on literature data (see text for references). For these samples, the uncertainty on the $\varepsilon_{Nd(T)}$ composition is ~0.9 ε-units, reflecting the 2σ variation of the literature $^{147}Sm/^{144}Nd$ values. For samples SM_2 and CH_2, for which measured $^{147}Sm/^{144}Nd$ ratios are available, the uncertainty is ~0.4 ε-units. Nd standard reproducibilities and blanks are given in the text.

4. Results

4.1. Oxygen isotopes

Throughout the Early Jurassic, $\delta^{18}O_{apatite}$ values show a relatively large range from 17.3 to 22.5‰ (Fig. 4A). Pelagic fish teeth display quite high $\delta^{18}O$ values of 21.1‰ during the Hettangian (Liasicus Zone) and slightly lower values around 20.4‰ at the onset of the Late Pliensbachian (Margaritatus Zone; Stokesi Subzone). The end of the Late Pliensbachian is characterized by markedly higher $\delta^{18}O$ values (~22‰ during the Spinatum Zone; Hawskerense Subzone). During the Early Toarcian, pelagic fish tooth $\delta^{18}O$ rapidly decreases to a minimum value of ~17.5‰ at the base of the Falciferum Zone (Exaratum Subzone). The trend is reversed during the Bifrons Zone (Crassum Subzone) and $\delta^{18}O$ reaches around 19.3‰, before slightly decreasing to ~19‰ during the Aalensis Zone. Demersal fish remains display a similar range in $\delta^{18}O$, except during the Crassum Subzone where average values of 20.4‰ are recorded and during the Aalensis Zone where teeth of a demersal ray yielded a lower $\delta^{18}O$ value of 17.5‰. The decrease in $\delta^{18}O$ from the Early to Middle Toarcian is also recorded by the nektobenthic fishes.

Similarly to the fish tooth data, belemnite $\delta^{18}O$ values decrease at the Pliensbachian–Toarcian boundary, from a maximum of ~0.5‰ during the Spinatum Zone to a minimum of −2.5‰ during the Falciferum Zone. During the Bifrons Zone (Crassum Subzone), the belemnite data display a relatively large variability of about 2.5‰, with an average value of −1.5‰.

4.2. Neodymium isotopes

The initial ε_{Nd} values of fish teeth from Euro-boreal areas vary through the Early Jurassic with values ranging from −6.2 to −10.5 (Fig. 4B and Table 3). The single value obtained for the Sinemurian (Semicostatum Zone) is quite unradiogenic and reaches −9.1 ε-units. During the Pliensbachian, fish tooth ε_{Nd} values are still unradiogenic (−9.3 to −10), except at the end of the Davoei Zone and at the beginning of the Margaritatus Zone, where a significant positive excursion (−6.2 and −6.9) is recorded. During the Toarcian, available ε_{Nd} data are between −9.1 and −10, and show a minimum value of −10.5 ε-units during the Falciferum Zone (Exaratum Subzone).

5. Discussion

5.1. $\delta^{18}O$ variations through the Early Jurassic

5.1.1. Comparison of biological materials

We compiled a low-latitude composite $\delta^{18}O$ curve (based on belemnite, oyster, and brachiopod $\delta^{18}O$ data from several European sections) for the Early Jurassic period, using the Pliensbachian–Toarcian database of Dera et al. (2009) and additional literature data

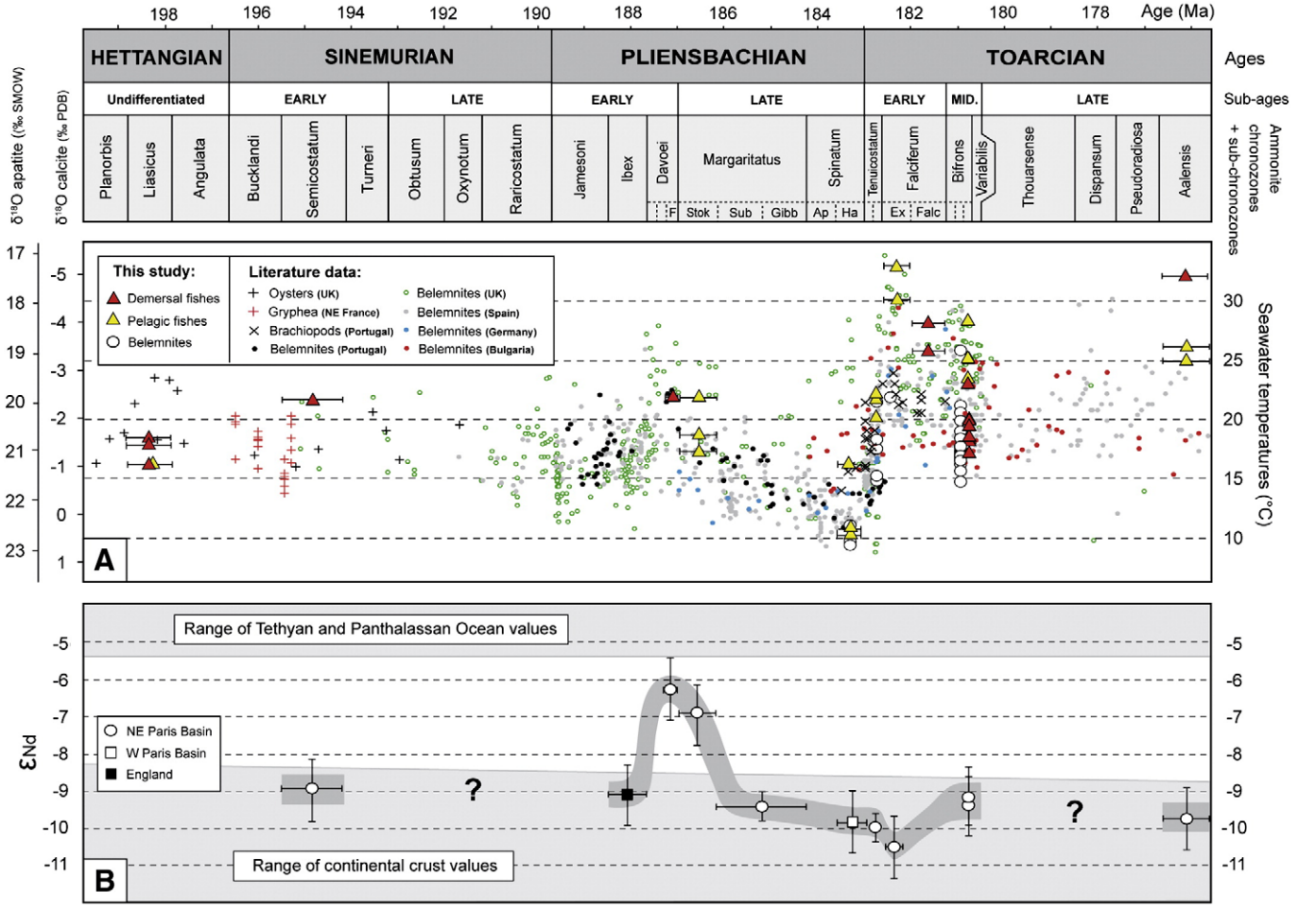

Fig. 4. Variations of $\delta^{18}O$ and ε_{Nd} through the Early Jurassic. (A) Comparison of bivalve, brachiopod, belemnite and fish tooth $\delta^{18}O$ records and calculated paleotemperatures. $\delta^{18}O$ records from Hesselbo et al. (2000b), McArthur et al. (2000), Jenkyns et al. (2002), Bailey et al. (2003), Nori and Lathuilière (2003), Rosales et al. (2004), van de Schootbrugge et al. (2005a), Gómez et al. (2008), Metodiev and Koleva-Rekalova (2008) and Suan et al. (2008). $\delta^{18}O$ data have been calibrated to the ammonite biozone resolution using the absolute ages of chronozone boundaries defined by Gradstein et al. (2004). $\delta^{18}O$ data points for belemnites from the Bifrons Zone contemporaneous with fish tooth data points were slightly shifted to the left for graphical clarity. (B) ε_{Nd} variations through the Early Jurassic. ε_{Nd} ranges for continental crust, Tethys and Panthalassa seawater are from Stille et al. (1996).

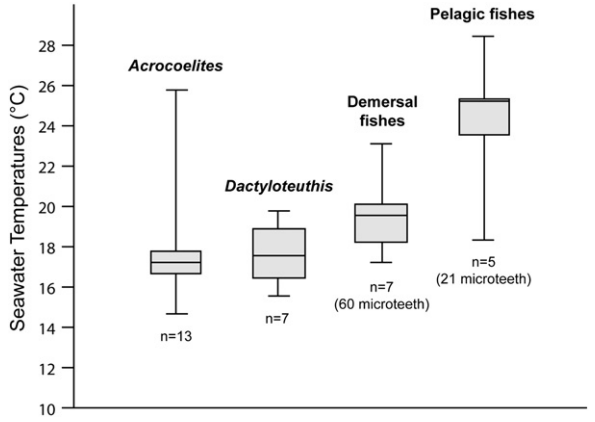

Fig. 5. Comparison of temperatures inferred from $\delta^{18}O$ values recorded by belemnites (*Acrocoelites* and *Dactyloteuthis* genera), pelagic fishes, and demersal fishes recovered from the same bed of the Bifrons Zone (Crassum Subzone). Horizontal lines, boxes and vertical lines indicate medians, quartiles, and maximal ranges, respectively.

from Jenkyns et al. (2002), Nori and Lathuilière (2003), and Metodiev and Koleva-Rekalova (2008) (Fig. 4A). Oxygen isotope values of fish tooth apatite and belemnite calcite analysed in this study along with literature data were converted into temperatures, using the equations of Kolodny et al. (1983) and Anderson and Arthur (1983), respectively, and assuming a $\delta^{18}O_{seawater}$ equal to −1‰ for an ice-free period (Shackleton and Kennett, 1975). Throughout the studied interval, analysed fish teeth and belemnite rostra display similar trends in $\delta^{18}O$ with both records in accordance with the Early Jurassic $\delta^{18}O$ composite curve. This correspondence between the $\delta^{18}O$ of biogenic apatite and calcite suggests that the recorded variations represent a paleoenvironmental signal and that a bias related to the ecology of belemnites is not of major importance.

In order to compare the temperatures derived from different belemnite genera, demersal and pelagic fish teeth, a Kruskall–Wallis non-parametric test was performed on samples recovered from a single horizon of the Crassum Subzone (Bifrons Zone). This level is particularly suitable due to the high abundance of belemnites and fish teeth. The results demonstrate that, during the Bifrons Zone, temperatures inferred from pelagic fish are significantly different from the temperatures calculated from demersal fish teeth and belemnites ($p<0.01$), which can be explained by different life habitats (e.g., Picard et al., 1998) (Fig. 5). Temperatures recorded by the belemnites *Acrocoelites*, *Dactyloteuthis* and bottom dwelling fishes are about 6 to 8 °C cooler than those recorded by pelagic fishes mainly inhabiting near-surface waters, and yielding temperatures of about ~23–26 °C. This implies that both belemnite genera and the demersal fishes lived at similar depths and in deeper water environments than the pelagic fishes. Our data therefore corroborate the nektobenthic habitat of belemnites, already suggested by van de Schootbrugge et al. (2000), Dutton et al. (2007), McArthur et al. (2007), and Wierzbowski and Joachimski (2007). However, such a temperature difference between nektobenthic and near-surface organisms is not systematically observed throughout the Early Jurassic. For example, during the Aalensis Zone, the temperature recorded by a demersal ray is higher (32 °C) than those inferred from three coeval pelagic fish samples (25–26 °C). In addition, temperatures given by bottom and surface swimmers are very similar during the Spinatum Zone (2.5 °C of difference), but gradually diverge during the Early Toarcian, and reach a difference of ~6 °C during the first-order maximum flooding of the Bifrons Zone (Hardenbol et al., 1998) (Fig. 6). As this offset increases during the Early–Middle Toarcian transgressive event (Hallam, 1981), we suggest that this pattern could reflect an increasing difference between surface and bottom water temperatures linked to deepening during platform flooding. Conversely, during lowstand sea-level periods (e.g., Spinatum Zone), the surface-bottom water temperature difference would not be sufficient in the NW Tethyan epicontinental seas to clearly discern differences in temperatures inferred from organisms with different ecological behaviours.

5.1.2. Evolution of seawater temperatures

Hettangian–Sinemurian fish tooth $\delta^{18}O$ data yield low seawater temperatures (16 to 18.5 °C) during the Liasicus Zone and a warmer temperature (21.7 °C) during the Semicostatum Zone. Data are scarce but are similar to that displayed by bivalve shells (Jenkyns et al., 2002; Nori and Lathuilière, 2003), which are interpreted to be reliable recorders of seawater temperature (Brigaud et al., 2008). Reconstructed temperatures inferred from fish teeth reach a maximum at the Davoei–Margaritatus Zone transition (17–23 °C) coeval with the Early Pliensbachian warming documented by the $\delta^{18}O$ composite curve. Temperatures decrease to 10 °C during the Spinatum Zone which are similar to temperatures reconstructed from belemnite $\delta^{18}O$ (this study). Such temperatures appear surprisingly cold for low latitudes. However, part of the $\delta^{18}O$ increase recorded by belemnites and fish teeth may arise from the growth of limited ice-caps, as suggested by the occurrence of glendonite in Siberia during the Pliensbachian (Price, 1999). If ice-sheets were present during the Spinatum Zone, calculated temperatures would be higher than 10 °C.

At the Pliensbachian–Toarcian boundary, fish, belemnite, and brachiopod isotope data highlight a significant decrease in $\delta^{18}O$, reaching a minimum during the Early Toarcian Oceanic Anoxic Event (Exaratum Subzone, Falciferum Zone). The maximum decrease of ~5.5‰ is recorded by pelagic fish from the Paris Basin and belemnites from Yorkshire, corresponding to a temperature rise of ~20 °C during an interval of 1 My if explained solely in terms of temperature. Such a warming appears unrealistic, especially for low latitudes (~30°N). An increased freshwater influx during the Falciferum Zone may have resulted in a lowering of both salinity and $\delta^{18}O$ of NW Tethyan seawater and may thus account for part of the shift in $\delta^{18}O$ (Saelen et al., 1996; Bailey et al., 2003; Suan et al., 2008). This interpretation is in agreement with a coeval positive osmium isotope excursion recorded in Yorkshire, which is interpreted to reflect an intensification of the continental weathering at global scale (Cohen et al. 2004) or massive riverine inputs in Euro-boreal domains that could have been enhanced by the marine restriction of basins (McArthur et al. 2008).

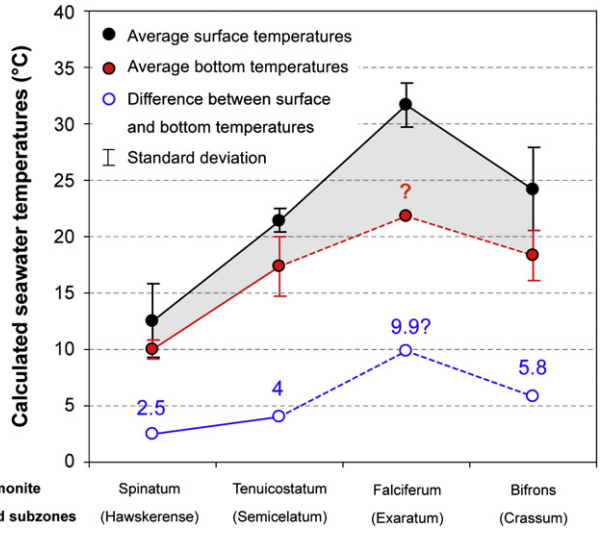

Fig. 6. Divergences between surface and bottom seawater temperatures at the Pliensbachian–Toarcian boundary. Average surface temperatures are inferred from $\delta^{18}O$ data of pelagic fishes whereas bottom temperatures are calculated using $\delta^{18}O$ of belemnites and demersal fishes. Note that, during the Exaratum Subzone, the difference is very important but may be biased by the poor sampling of bottom organisms (i.e., one belemnite) or by strong freshwater runoff affecting surface waters.

Alternatively, the Early Toarcian sea-level rise may have resulted in an increasing contribution of Arctic waters into the NW Tethys through the Viking Corridor and a lowering of seawater $\delta^{18}O$ in the Euro-Boreal domain, and to a lesser extent in the Mediterranean area. Even in an ice-free world, Arctic waters are indeed expected to have lower salinities and lower $\delta^{18}O$ signatures, due to freshwater inputs derived from high-latitude precipitation, characterized by a markedly low $\delta^{18}O$, and to limited deep water mass exchanges with other oceanic basins (Rozanski et al., 1993). Both scenarios imply that the calculation of temperatures using a constant $\delta^{18}O_{seawater}$ would result in an overestimation of the Early Toarcian warming.

Our data show a temperature decrease from the Falciferum (Falciferum Subzone) to the Bifrons Zone (Crassum Subzone) corroborating the general trend displayed by belemnite $\delta^{18}O$ values from Yorkshire and Spain (McArthur et al., 2000; Gómez et al., 2008). During the Aalensis Zone, the temperatures inferred from demersal and pelagic fishes are between 25 and 32 °C and are thus slightly higher than those inferred from belemnite $\delta^{18}O$ records from Spain and Bulgaria (Gómez et al., 2008; Metodiev and Koleva-Rekalova, 2008).

5.2. Early Jurassic ε_{Nd} variations in Euro-boreal seas — implications for temperature and salinity variations

Fish tooth apatite inherits its Nd isotope composition quite rapidly at the sediment–water interface (Bernat, 1975; Martin and Scher, 2004) by recording the isotope signal of bottom waters without any apparent isotope fractionation (Martin and Haley, 2000). Neodymium is supplied to the ocean through continental weathering. Differences in age and lithologic composition (crustal *vs.* mantle) of weathered rocks surrounding the oceanic basins result in interbasinal differences in ε_{Nd} values which are retained because of the short residence time of Nd (~500 yr) relative to ocean mixing (Piepgras and Wasserburg, 1980; Tachikawa et al., 2003). As fish teeth record the ε_{Nd} signature of seawater at the bottom of the water column and as the analysed samples have been deposited in relatively shallow seas (maximum 200 m water depth), we expect fish teeth to record the ε_{Nd} composition of Euro-boreal upper ocean waters. The ε_{Nd} variations recorded in an oceanic basin may be related to (i) changes in the relative weathering rates of exposed old crustal *vs.* young volcanic rocks (ii) changes in water circulation between isotopically different ocean basins as a consequence of variations in sea level or tectonic movements (Stille et al., 1996; Reynolds et al., 1999; Von Blackenburg and Nägler, 2001; Scher and Martin, 2004; Pucéat et al., 2005).

Except during the Pliensbachian positive shift, ε_{Nd} of Euro-boreal water masses was relatively low (−10 to −9) and compares relatively well with values reported by Négrel et al. (2006) for the Middle and Late Jurassic from the Paris Basin. The similarity of the values with those of the contemporaneous average continental crust (−8.5 to −12; Stille and Fisher, 1990) points to a dominant influence of unradiogenic Nd inputs from the weathering of surrounding emerged areas (Fig. 4B). As illustrated by paleophytogeography (Rees et al., 2000), clay mineral distribution (Dera et al., 2009), and simulations using General Circulation Models (GCM) (Chandler et al., 1992), this is in agreement with humid climatic conditions in the mid-latitudes favouring a strong runoff and freshwater discharge. However, as boreal-arctic waters are likely to have been quite unradiogenic due to Nd inputs from weathering of Paleozoic and Precambrian continental rocks exposed on the Fenno-Scandian shield (Pucéat et al., 2005), boreal water masses could have contributed to the unradiogenic signature of Euro-boreal waters. Importantly, the unradiogenic values imply a limited influence of eastern Tethyan and Panthalassan waters in the Euro-boreal domains during most of the Early Jurassic. The ε_{Nd} signature of these water masses has remained more radiogenic over the Jurassic period (−1 to −5.5 ε-units) due to weathering of island-arc related materials (Keto

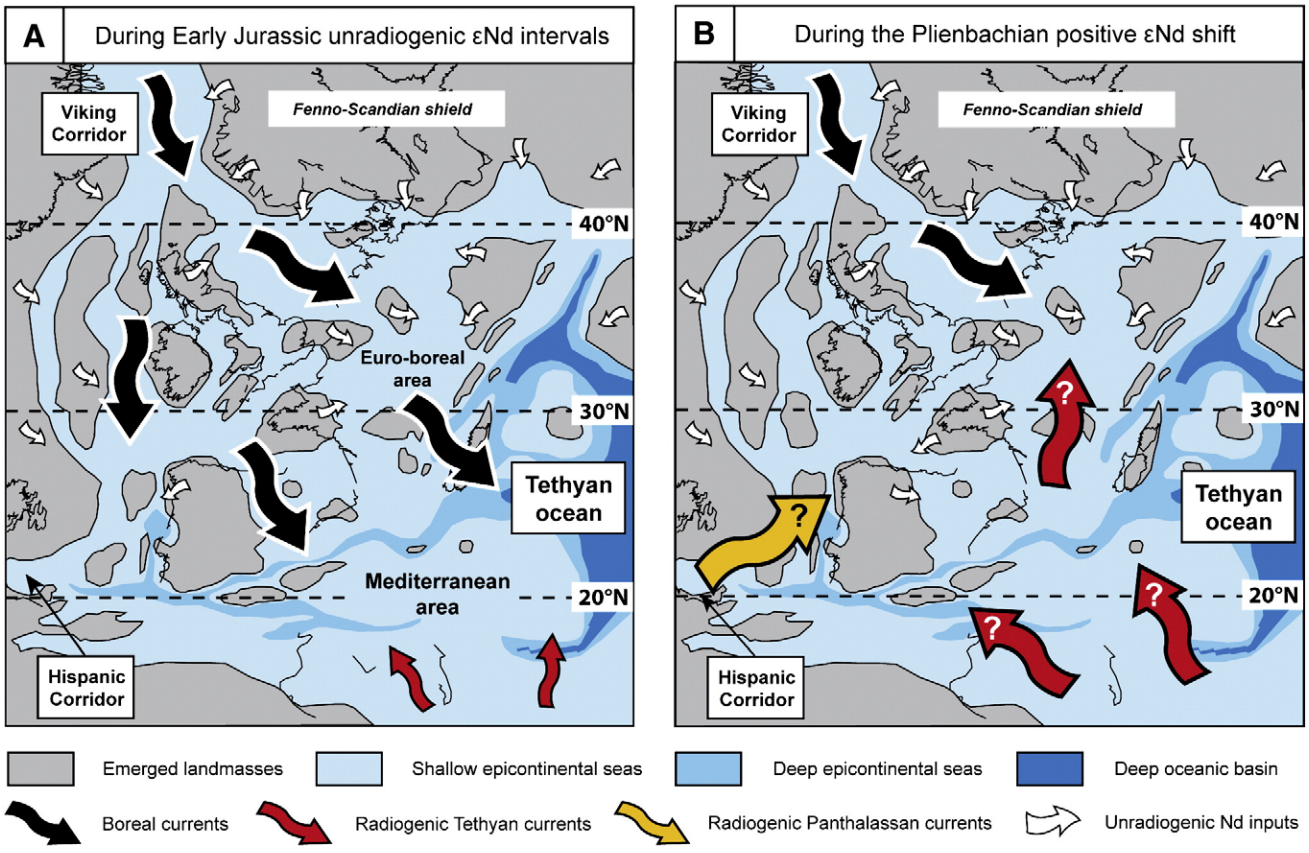

Fig. 7. Schematic representation of the main surface currents during (A) the Early Jurassic unradiogenic ε_{Nd} intervals and (B) the Pliensbachian positive ε_{Nd} excursion. Paleogeographic maps modified after Thierry et al. (2000).

and Jacobsen, 1988; Stille et al., 1996). Our data therefore support the presence of dominant southward currents during most of the Early Jurassic (Fig. 7A), as simulated by Bjerrum et al. (2001).

5.2.1. Warming and circulation changes during the Pliensbachian

At the end of the Early Pliensbachian (Davoei Zone), Euro-boreal waters show a positive excursion in ε_{Nd} (up to −6) (Fig. 4B). As the abundance of kaolinite in sediments and strontium isotope ratios point to more humid climatic conditions in the NW Tethys during this interval (Dera et al., 2009), we argue that the change in ε_{Nd} cannot be related to a reduction of unradiogenic continental Nd discharges. Instead, we suggest that the shift in neodymium isotopes results from a change in the oceanic circulation. More specifically, we propose a northward incursion of radiogenic eastern Tethyan or Panthalassan waters into the Euro-boreal areas during the Davoei Zone and at the onset of the Margaritatus Zone (Fig. 7B). This scenario is corroborated by coeval biotic events such as incursions of Tethyan ostracods into the northern European basins (Arias, 2006) and an increasing diversity of Mediterranean ammonites in Euro-boreal domains (Dommergues and Meister, 1991). In addition, the first occurrence of Panthalassan bivalves in NW Tethyan domains is reported during the Margaritatus Zone, which has been related to the opening of the Hispanic Corridor linking the Panthalassa and NW Tethys (Aberhan, 2001). However, as both the Panthalassa and Tethys oceans have a radiogenic signature which is not isotopically distinct before the Middle Jurassic (Stille et al., 1996), it is not possible to differentiate the respective influence of these two water masses on Euro-boreal waters.

Interestingly, the positive shift in ε_{Nd} is coeval with the warming inferred from $\delta^{18}O$ data during the Davoei Zone (Fig. 4). We suspect that northward incursions of warm and more radiogenic waters from the Tethys or Panthalassa may have contributed to the recorded warming in the Euro-boreal region. This currentologic change may be explained by three different processes:

1. It could be due to a regional deepening of Mediterranean basins, favouring the transfer of low latitude water masses into Euro-boreal areas. Indeed, during the Early Pliensbachian, numerous block tilting events related to the Tethyan and mid-Atlantic rifting have been reported on the northern Gondwanan margin (Lachkar et al., 2009). These block tilting could have enhanced connections between Mediterranean basins.
2. The incursion of warm and radiogenic currents could be related to the opening of the narrow and shallow Hispanic Corridor, with an increasing influence of seawater from the eastern equatorial area of the Panthalassan Ocean.
3. Finally, a global warming event may have induced regional perturbation of currentologic circulations.

5.2.2. Increased runoff at the Pliensbachian/Toarcian transition

The marked decrease in $\delta^{18}O$ during the Falciferum Zone (Exaratum Subzone) is not associated with a significant variation of seawater ε_{Nd}. More specifically, the lack of a large negative ε_{Nd} excursion argues against a massive influx of Arctic waters through the Viking Corridor during the Early Toarcian sea-level rise as we expect these waters to have been even less radiogenic due to the contribution of Nd from nearby exposed crustal rocks (e.g., $\varepsilon_{Nd} = -17$ for a Cretaceous fish tooth from Sweden; Pucéat et al., 2005). We therefore argue that enhanced runoff during the Falciferum Zone may in part explain the recorded decrease of $\delta^{18}O$. Because Euro-boreal waters already had a low ε_{Nd} signature comparable to that of the contemporaneous continental crust during most of the Early Jurassic (Stille and Fisher, 1990; Fig. 4B), massive discharges of Nd from continental areas are expected to have had only a minor influence on the Nd isotope composition of the local seawater.

Interestingly, the amplitude of $\delta^{18}O$ excursions recorded by belemnites, brachiopods, and fish teeth at the Plienbachian–Toarcian transition is higher in northern latitudes and decreases toward the South (Fig. 4A and Appendix A). The range of $\delta^{18}O$ fluctuations reaches 6 to 5.5‰ in Yorkshire (McArthur et al., 2000; Jenkyns et al., 2002) and in the Paris Basin (this study), ~3.5 to 3‰ in Bulgaria (Metodiev and Koleva-Rekalova, 2008) and in South Germany (Bailey et al., 2003), ~3.5 to 3‰ in central and northern Spain (Rosales et al., 2004; van de Schootbrugge et al., 2005a; Gómez et al., 2008) and ~2.5‰ in Portugal (Suan et al., 2008). This general decrease suggests that, at the Pliensbachian–Toarcian transition, freshwater runoff was stronger in the north-western areas and gradually decreased southward. As suggested McArthur et al. (2008), the basinal restriction of Euro-boreal domains could also have favoured a local drop of salinity in surface seawaters.

6. Conclusion

New oxygen and neodymium isotope analyses performed on biostratigraphically well-dated fish remains and belemnites from the Paris Basin allow us to develop a better understanding of the origin of Early Jurassic $\delta^{18}O$ variations previously determined from belemnites, oysters and brachiopods. The presented oxygen isotope records show a strong correspondence between $\delta^{18}O$ variations recorded by fish tooth apatite and belemnite calcite, confirming the paleoenvironmental significance of the $\delta^{18}O$ trends. The oxygen isotope composition of both organisms indicates warm seawater temperatures at the end of the Early Pliensbachian, cooling during the Late Pliensbachian, and significant warming during the Early Toarcian. Temperatures recorded by pelagic fishes and nektobenthic organisms (i.e., belemnites and demersal fishes) display a small difference (~2.5 °C) during the sea-level lowstand of the Spinatum Zone but gradually diverged (~6 °C) during the Early–Middle Toarcian transgression. We therefore suggest that, during regressive phases, the temperature difference between surface and bottom waters was too small to be recorded by organisms having different life habitats.

The globally unradiogenic Nd composition of Euro-boreal waters through the Early Jurassic suggests that these waters received neodymium inputs by weathering of surrounding landmasses with only a limited influence of more radiogenic Tethyan and Panthalassan waters. As suggested by modelling experiments, this supports the existence of southward currents in the Euro-boreal area during most of the Early Jurassic. Nevertheless, a positive excursion recorded between the Davoei and Margaritatus Zones suggests a temporary incursion of low-latitude Tethyan or Panthalassan waters into the northern areas, which may have contributed to the seawater warming recorded during this interval.

During the Falciferum Zone, the absence of a marked ε_{Nd} negative excursion associated with the negative $\delta^{18}O$ shift recorded by different organisms argues against the influence of unradiogenic Arctic waters characterized by very low $\delta^{18}O$ values. Our data are in better agreement with an enhanced input of isotopically light freshwaters related to increased weathering that could have contributed to the large $\delta^{18}O$ shift recorded by belemnites, fish teeth and brachiopods.

Acknowledgements

This paper is a contribution of the SEDS "Système, Environnements, et Dynamique Sédimentaire" and FED "Forme, Évolution, Diversité" teams of the CNRS Biogéosciences laboratory. The International Association of Sedimentologists (IAS) is highly acknowledged for the financial support credited through a postgraduate grant awarded in 2007. We are grateful to J. Rees for tooth samples from England, and thank Daniele Lutz, Christiane Parmentier, and Catherine Zimmermann for technical assistance in the laboratory. Finally, P. Delaney, B. van de Schootbrugge, and an anonymous reviewer are thanked for their constructive remarks which improved the manuscript.

Appendix A. Supplementary data

Supplementary data associated with this article can be found, in the online version, at 10.1016/j.epsl.2009.06.027.

References

Aberhan, M., 2001. Bivalve palaeobiogeography and the Hispanic Corridor: time of opening and effectiveness of a proto-Atlantic seaway. Palaeogeogr. Palaeoclimatol. Palaeoecol. 165, 375–394.

Anderson, T.F., Arthur, M.A., 1983. Stable isotopes of oxygen and carbon and their application to sedimentologic and paleoenvironmental problems. In: Arthur, M.A., Anderson, T.F., Kaplan, I.R., Veizer, J., Land, L.S. (Eds.), Stable Isotopes in Sedimentary Geology. SEPM Short Course, 10. Tulsa, pp. 1–151.

Arias, C., 2006. Northern and southern hemispheres ostracod palaeobiogeography during the Early Jurassic: possible migration routes. Palaeogeogr. Palaeoclimatol. Palaeoecol. 233, 63–95.

Bailey, T.R., Rosenthal, Y., McArthur, J.M., van de Schootbrugge, B., Thirwall, M.F., 2003. Paleoceanographic changes of the Late Pliensbachian–Early Toarcian interval: a possible link to the genesis of an Oceanic Anoxic Event. Earth Planet. Sci. Lett. 212, 307–320.

Beerling, D.J., Lomas, M.R., Gröcke, D.R., 2002. On the nature of methane gas–hydrate dissociation during the Toarcian and the Aptian oceanic anoxic event. Am. J. Sci. 302, 28–49.

Bernat, M., 1975. Les isotopes de l'uranium et du thorium et les terres rares dans l'environnement marin. Cah. ORSTOM Ser. Geol. 7, 65–83.

Bjerrum, C.J., Surlyk, F., Callomon, J.H., Slingerland, R.L., 2001. Numerical paleoceanographic study of the Early Jurassic transcontinental Laurasian Seaway. Paleoceanography 16, 390–404.

Boulvain, F., Belanger, I., Ghysel, P., Laloux, M., Roche, M., Delsate, D., Dosquet, D., Teerlynck, H., Thorez, J., Godefroit, P., 2000. New lithostratigraphical, sedimentological, mineralogical and palaeontological data on the Mesozoic of Belgian Lorraine: a progress report. Geol. Belg. 3, 3–33.

Brigaud, B., Pucéat, E., Pellenard, P., Vincent, B., Joachimski, M.M., 2008. Climatic fluctuations and seasonality during the Late Jurassic (Oxfordian–Early Kimmeridgian) inferred from $\delta^{18}O$ of Paris Basin oyster shells. Earth Planet. Sci. Lett. 273, 58–67.

Cappetta, H., 1987. Mesozoic and Cenozoic Elasmobranchii, Chondrichthyes II. In: Schultze, H.P. (Ed.), Handbook of Paleoichthyology (vol. 3B). Gustav Fischer, New York.

Chandler, M.A., Rind, D., Ruedy, R., 1992. Pangean climate during the Early Jurassic: GCM simulations and the sedimentary record of paleoclimate. Geol. Soc. Am. Bull. 104, 543–559.

Cohen, A.S., Coe, A.L., Harding, S.M., Schwark, L., 2004. Osmium isotope evidence for the regulation of atmospheric CO_2 by continental weathering. Geology 32, 157–160.

Damborenea, S.E., 2002. Jurassic evolution of Southern Hemisphere marine palaeobiogeographic units based on benthonic bivalves. Geobios Mém. Spec. 35 (24), 51–71.

Delsate, D., 2003. Une nouvelle faune de poissons et requins Toarciens du sud du Luxembourg (Dudelange) et de l'Allemagne (Schömberg). Bull. Acad. Lorraine Sci. 42, 13–49.

Dera, G., Pellenard, P., Neige, P., Deconinck, J.-F., Pucéat, E., Dommergues, J.L., 2009. Distribution of clay minerals in Early Jurassic Peritethyan seas: palaeoclimatic significance inferred from multiproxy comparisons. Palaeogeogr. Palaeoclimatol. Palaeoecol. 271, 39–51.

Dommergues, J.-L., Meister, C., 1991. Area of mixed marine faunas between two major paleogeographical realms, exemplified by the Early Jurassic (Late Sinemurian and Pliensbachian) ammonites in the Alps. Palaeogeogr. Palaeoclimatol. Palaeoecol. 86, 265–282.

Doyle, P., 1990. The British Toarcian (Lower Jurassic) belemnites. Part 1. Monograph of the Palaeontographical Society, London, pp. 1–49. pls 1–17.

Doyle, P., 1994. Aspects of the distribution of Lower Jurassic belemnites. Palaeopelagos 1, 109–121.

Dutton, A., Huber, B.T., Lohmann, K.C., Zinsmeister, W.J., 2007. High-resolution stable isotope profiles of dimitobelid belemnite: implications for paleodepth habitat and Late Maastrichtian climate seasonality. Palaios 22, 642–650.

Gómez, J.J., Goy, A., Canales, M.L., 2008. Seawater temperature and carbon isotope variations in belemnites linked to mass extinction during the Toarcian (Early Jurassic) in Central and Northern Spain. Comparison with other European sections. Palaeogeogr. Palaeoclimatol. Palaeoecol. 258, 28–58.

Gradstein, F.M., Ogg, J.G., Smith, A.G., 2004. A Geologic Time Scale 2004. Cambridge University Press, Cambridge.

Grandjean, P., Cappetta, H., Michard, A., Albarède, F., 1987. The assessment of REE patterns and $^{143}Nd/^{144}Nd$ ratios in fish remains. Earth Planet. Sci. Lett. 84, 181–196.

Grandjean, P., Cappetta, H., Albarède, F., 1988. The REE and ε_{Nd} of 40–70 Ma old fish debris from the west-African platform. Geophys. Res. Lett. 15, 389–392.

Hallam, A., 1981. A revised sea-level curve for the Early Jurassic. J. Geol. Soc. London 138, 735–743.

Hardenbol, J., Thierry, J., Farley, M.B., de Graciansky, P.-C., Vail, P.R., 1998. Mesozoic and Cenozoic sequence chronostratigraphic framework of European basins. In: de Graciansky, P.-C., Hardenbol, J., Jacquin, T., Vail, P.R. (Eds.), Mesozoic and Cenozoic Sequence Stratigraphy of European Basins, Special Publication, vol. 60. Society for Sedimentary Geology, pp. 3–13.

Hermoso, M., Le Callonnec, L., Minoletti, F., Renard, M., Hesselbo, S., 2009. Expression of the Early Toarcian negative carbon-isotope excursion in separated carbonate microfractions (Jurassic, Paris Basin). Earth Planet. Sci. Lett. 277, 194–203.

Hesselbo, S.P., Gröcke, D.R., Jenkyns, H.C., Bjerrum, C.J., Farrimond, P., Morgans-Bell, H.S., Green, O.R., 2000a. Massive dissociation of gas hydrates during a Jurassic oceanic anoxic event. Nature. 406, 392–395.

Hesselbo, S.P., Meister, C., Gröcke, D.R., 2000b. A potential global stratotype for the Sinemurian–Pliensbachian boundary (Lower Jurassic), Robin Hood's Bay, UK: ammonite faunas and isotope stratigraphy. Geol. Mag. 137, 601–607.

Hesselbo, S.P., Jenkyns, H.C., Duarte, L.V., Oliveira, L.C.V., 2007. Carbon-isotope record of the Early Jurassic (Toarcian) oceanic anoxic event from fossil wood and marine carbonate (Lusitanian Basin, Portugal). Earth Planet. Sci. Lett. 253, 455–470.

Jenkyns, H.C., 1988. The early Toarcian (Jurassic) anoxic event: stratigraphic, sedimentary, and geochemical evidence. Am. J. Sci. 288, 101–151.

Jenkyns, H.C., Jones, C.E., Gröcke, D.R., Hesselbo, S.P., Parkinson, D.N., 2002. Chemostratigraphy of the Jurassic System: applications, limitations and implications for palaeoceanography. J. Geol. Soc. 159, 351–378.

Joachimski, M.M., Van Geldem, R., Breisig, S., Buggisch, W., Day, J., 2004. Oxygen isotope evolution of biogenic calcite and apatite during the Middle and Late Devonian. Int. J. Earth Sci. 93, 542–553.

Jones, C.E., Halliday, A.N., Rea, D.K., Owen, R.M., 1994. Neodymium isotopic variations in north pacific modern silicate sediment and the insignificance of detrital REE contributions to seawater. Earth Planet. Sci. Lett. 127, 55–66.

Keto, L.S., Jacobsen, S.T., 1988. Nd isotopic variations of Phanerozoic paleoceans. Earth Planet. Sci. Lett. 90, 395–410.

Kolodny, Y., Luz, B., Navon, O., 1983. Oxygen isotope variations in phosphate of biogenic apatites, I. Fish bone apatite-rechecking the rules of the game. Earth Planet. Sci. Lett. 64, 398–404.

Lachkar, N., Guiraud, M., El Harfi, A., Dommergues, J.-L., Dera, G., Durlet, C., 2009. Early Jurassic normal faulting in a carbonate extensional basin: characterization of tectonic-driven platform drowning (central High Atlas rift, Morocco). J. Geol. Soc. 166, 413–430.

Lécuyer, C., Grandjean, P., Sheppard, S.M.F., 1999. Oxygen isotope exchange between dissolved phosphate and water at temperatures $\leq 135\,^{\circ}C$: inorganic versus biological fractionations. Geochim. Cosmochim. Acta 63, 855–862.

Lécuyer, C., Reynard, B., Grandjean, P., 2004. Rare earth element evolution of Phanerozoic seawater recorded in biogenic apatites. Chem. Geol. 204, 63–102.

Little, C.T.S., Benton, M.J., 1995. Early Jurassic mass extinction: a global long-term event. Geology 23, 495–498.

Martin, E.E., Haley, B.A., 2000. Fossil fish teeth as proxies for seawater Sr and Nd isotopes. Geochim. Cosmochim. Acta 64, 835–847.

Martin, E.E., Scher, H.D., 2004. Preservation of seawater Sr and Nd isotopes in fossil fish teeth: bad news and good news. Earth Planet. Sci. Lett. 220, 25–39.

McArthur, J.M., Donovan, D.T., Thirlwall, M.F., Fouke, B.W., Mattey, D., 2000. Strontium isotope profile of the early Toarcian (Jurassic) oceanic anoxic event, the duration of ammonite biozones, and belemnite palaeotemperatures. Earth Planet. Sci. Lett. 179, 269–285.

McArthur, J.M., Doyle, P., Leng, M.J., Reeves, K., Williams, C.T., Garcia-Sanchez, R., Howarth, R.J., 2007. Testing palaeo-environmental proxies in Jurassic belemnites: Mg/Ca, Sr/Ca, Na/Ca, $\delta^{18}O$ and $\delta^{13}C$. Palaeogeogr. Palaeoclimatol. Palaeoecol. 252, 464–480.

McArthur, J.M., Algeo, T.J., van de Schootbrugge, B., Li, Q., Howarth, R.J., 2008. Basinal restriction, black shales, Re–Os dating, and the Early Toarcian (Jurassic) oceanic anoxic event. Paleoceanography 23, PA4217.

McElwain, J.C., Wade-Murphy, J., Hesselbo, S.P., 2005. Changes in carbon dioxide during an oceanic anoxic event linked to intrusion into Gondwana coals. Nature 435, 479–482.

Metodiev, L., Koleva-Rekalova, E., 2008. Stable isotope records ($\delta^{18}O$ and $\delta^{13}C$) of Lower–Middle Jurassic belemnites from the Western Balkan mountains (Bulgaria): palaeoenvironmental application. Appl. Geochem. 23, 2845–2856.

Négrel, P., Casanova, J., Brulhet, J., 2006. REE and Nd isotope stratigraphy of Late Jurassic carbonate platform, eastern Paris Basin, France. J. Sed. Res. 76, 605–617.

Nori, L., Lathuilière, B., 2003. Form and environment of *Gryphea arcuata*. Lethaia 36, 83–96.

O'Neil, J.R., Roe, L.J., Reinhard, E., Blake, R.E., 1994. A rapid and precise method of oxygen isotope analysis of biogenic phosphate. Isr. J. Earth Sci. 43, 203–212.

Picard, S., Lécuyer, C., Sheppard, S.M.F., Cappetta, H., Emig, C.C., 1998. Delta ^{18}O values of coexisting brachiopods and fish; temperature differences and estimates of paleowater depths. Geology 26, 975–978.

Picard, S., Lécuyer, C., Barrat, J.-A., Garcia, J.-P., Dromart, G., Sheppard, S.M.F., 2002. Rare earth element contents of Jurassic fish and reptile teeth and their potential relation to seawater composition (Anglo-Paris Basin, France and England). Chem. Geol. 186, 1–16.

Piepgras, D.J., Wasserburg, G.J., 1980. Neodymium isotopic variations in seawater. Earth Planet. Sci. Lett. 50, 128–138.

Price, G.D., 1999. The evidence and implications of polar ice during the Mesozoic. Earth-Sci. Rev. 48, 183–210.

Pucéat, E., Lécuyer, C., Reisberg, L., 2005. Neodymium isotope evolution of NW Tethyan upper ocean waters throughout the Cretaceous. Earth Planet. Sci. Lett. 236, 705–720.

Rees, J., 2000. A new Pliensbachian (Early Jurassic) neoselachian shark fauna from southern Sweden. Acta Palaeontol. Pol. 45, 407–424.

Rees, P.M., Ziegler, A.M., Valdes, P.J., 2000. Jurassic phytogeography and climates: new data and model comparisons. In: Huber, B.T., Macleod, K.G., Wing, S.L. (Eds.), Warm Climates in Earth history. Cambridge University Press, pp. 297–318.

Reynolds, B.C., Frank, M., O'Nions, R.K., 1999. Nd- and Pb-isotope time series from Atlantic ferromanganese crusts: implications for changes in provenance and paleocirculation over the last 8 Myr. Earth Planet. Sci. Lett. 173, 381–396.

Reynolds, B.C., Frank, M., Burton, K.W., 2006. Constraining erosional input and deep-water formation in the North Atlantic using Nd isotopes. Chem. Geol. 226, 253–263.

Röhl, H.J., Schmid-Röhl, A., Oschmann, W., Frimmel, A., Schwark, L., 2001. The Posidonia Shale (Lower Toarcian) of SW-Germany: an oxygen-depleted ecosystem controlled by sea level and palaeoclimate. Palaeogeogr. Palaeoclimatol. Palaeoecol. 165 (724), 27–52.

Rosales, I., Quesada, S., Robles, S., 2004. Paleotemperature variations of Early Jurassic seawater recorded in geochemical trends of belemnites from the Basque–Cantabrian basin, northern Spain. Palaeogeogr. Palaeoclimatol. Palaeoecol. 203, 253–275.

Rozanski, K., Araguas-Araguas, L., Gonfiantini, R., 1993. Isotopic patterns in modern global precipitation. In: Swart, P.K., Lohmann, K.C., McKenzie, J., Savin, S. (Eds.), Climate Change in Continental Isotopic Climate Records: Am. Geophys. Union, Geophys. Monogr., vol. 78, pp. 1–36.

Saelen, G., Doyle, P., Talbot, M.R., 1996. Stable-isotope analyses of belemnite rostra from the Whitby Mudstone Fm, England: surface water conditions during deposition of a marine black shale. Palaios 11, 97–117.

Scher, H.D., Martin, E.E., 2004. Circulation in the Southern Ocean during the Paleogene inferred from neodymium isotopes. Earth Planet. Sci. Lett. 228, 391–405.

Shackleton, N.J., Kennett, D.J., 1975. Paleotemperature history of the Cenozoic and initiation of Antarctic glaciation: oxygen and carbon isotope analyses in DSDP sites 277, 279 and 289. Init. Rep. Deep Sea Drill. Proj. 29, 743–755.

Stille, P., Fisher, H., 1990. Secular variation in the isotopic composition of Nd in Tethys seawater. Geochim. Cosmochim. Acta 54, 3139–3145.

Stille, P., Steinmann, M., Riggs, S.R., 1996. Nd isotope evidence for the evolution of the paleocurrents in the Atlantic and Tethys Oceans during the past 180 Ma. Earth Planet. Sci. Lett. 144, 9–19.

Suan, G., Mattioli, E., Pittet, B., Mailliot, S., Lécuyer, C., 2008. Evidence for major environmental perturbation prior to and during the Toarcian (Early Jurassic) oceanic anoxic event from the Lusitanian Basin, Portugal. Paleoceanography 23, PA1202.

Svensen, H., Planke, S., Chevallier, L., Malthe-Sørenssen, A., Corfu, F., Jamtveit, B., 2007. Hydrothermal venting of greenhouse gases triggering Early Jurassic global warming. Earth Planet. Sci. Lett. 256, 554–566.

Tachikawa, K., Athias, V., Jeandel, C., 2003. Neodymium budget in the modern ocean and paleo-oceanographic implications. J. Geophys. Res. 108, 10/1–10/3.

Thierry, J. et al., 2000. Middle Toarcian. In: Dercourt, J., Gaetani, M., Vrielynck, B., Barrier, E., Biju-Duval, B., Brunet, M.-F., Cadet, J.P., Crasquin, S., Sandulescu, M. (Eds.), Atlas Peri-Tethys Paleogeographical Maps, vol. I-XX.CCGM/CGMW, Paris, map 8, (40 co-authors).

Thomas, D.J., Bralower, T.J., Jones, C.E., 2003. Neodymium isotopic reconstruction of late Paleocene–early Eocene thermohaline circulation. Earth Planet. Sci. Lett. 209, 309–322.

van de Schootbrugge, B., Föllmi, K.B., Bulot, L.G., Burns, S.J., 2000. Paleoceanographic changes during the early Cretaceous (Valanginian–Hauterivian): evidence from oxygen and carbon stable isotopes. Earth Planet. Sci. Lett. 181, 15–31.

van de Schootbrugge, B., Bailey, T.R., Rosenthal, Y., Katz, M.E., Wright, J.D., Miller, K.G., Feist-Burkhardt, S., Falkowski, P.G., 2005a. Early Jurassic climate change and the radiation of organic-walled phytoplankton in the Tethys Ocean. Paleobiology 31, 73–97.

van de Schootbrugge, B., McArthur, J.M., Bailey, T.R., Rosenthal, Y., Wright, J.D., Miller, K.G., 2005b. Toarcian anoxic event: an assessment of global causes using belemnite C isotope records. Paleoceanography 21, PA3008.

Vennemann, T.W., Hegner, E., 1998. Oxygen, strontium, and neodymium isotope composition of fossil shark teeth as a proxy for the palaeoceanography and palaeoclimatology of the Miocene northern Alpine Paratethys. Palaeogeogr. Palaeoclimatol. Palaeoecol. 142, 107–121.

Vennemann, T.W., Hegner, E., Cliff, G., Benz, G.W., 2001. Isotopic composition of recent shark teeth as a proxy for environmental conditions. Geochim. Cosmochim. Acta 65, 1583–1599.

Vennemann, T.W., Fricke, H.C., Blake, R.E., O'Neil, J.R., Colman, A., 2002. Oxygen isotope analysis of phosphates: a comparison of techniques for analysis of Ag_3PO_4. Chem. Geol. 185, 321–336.

Von Blackenburg, F., Nägler, T.F., 2001. Weathering versus circulation-controlled changes in radiogenic isotope tracer composition of the Labrador Sea and north Atlantic deep water. Paleoceanography 16, 424–434.

Wierzbowski, H., Joackimski, M., 2007. Reconstruction of late Bajocian–Bathonian marine palaeoenvironments using carbon and oxygen isotope ratios of calcareous fossils from the Polish Jura Chain (central Poland). Palaeogeogr. Palaeoclimatol. Palaeoecol. 254, 523–540.

Zakharov, Y.D., Smyshlyaeva, O.P., Shigeta, Y., Popov, A.M., Zonova, T.D., 2006. New data on isotopic composition of Jurassic–Early Cretaceous cephalopods. Progress in Natural Science 16, 50–67.